

Supplementary Information

Controlled Synthesis of Up-Conversion NaYF₄:Yb,Tm Nanoparticles for Drug Release Under Near IR-Light Therapy

Edelweiss Moyano Rodríguez^{a,b}, Miguel Gomez-Mendoza^b, Raúl Pérez-Ruiz^{b,c}, Beatriz Peñín^d, Diego Sampedro^d, Antonio Caamaño^a, Víctor A. de la Peña O'Shea^b

[a] Signal theory and communications and telematic system and computing, Rey Juan Carlos University, Cam/ del Molin 5; 28942 Fuenlabrada, Madrid, Spain.

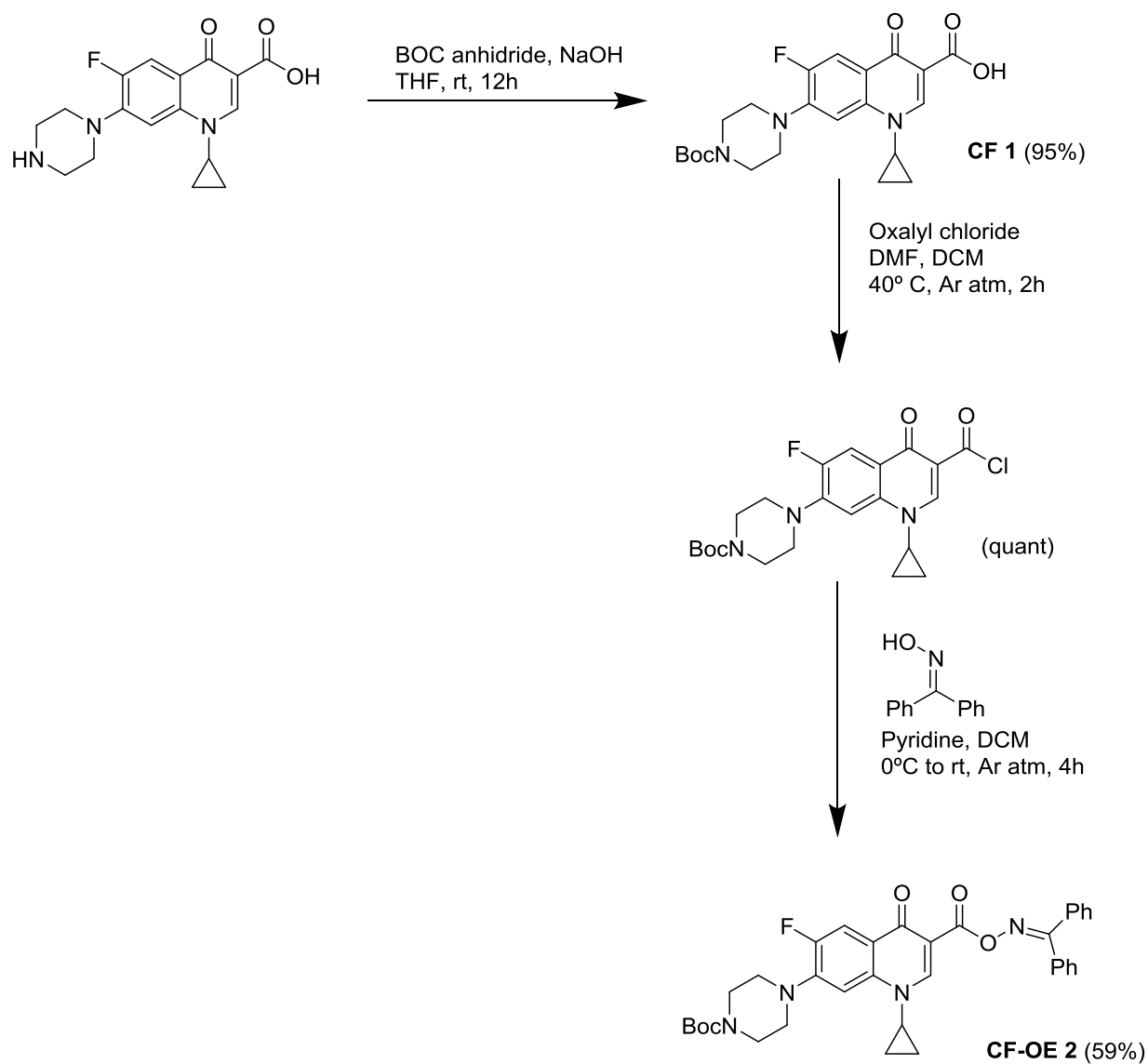
[b] Photoactivated Processes Unit IMDEA Energy Institute, C/ Ramón de la Sagra, 3 28935 Móstoles, Madrid, Spain.

[c] Departamento de Química, Universitat Politècnica de Valencia, Camno de Vera S/N, 46022, Valencia, Spain.

[d] Departamento de Química, Centro de Investigación en Síntesis Química (CISQ), Universidad de La Rioja, Madre de Dios, 53, 26006, Logroño, Spain.

Table of contents

Scheme S1. Synthetic route for the dyads CF (1) and CF-OE (2)	S3
Figure S1. ^1H (up) and ^{13}C (down) NMR of CF-OE 2	S4
Figure S2. Mass spectrometer characterization data of CF-OE 2	S5
Figure S3. TEM images of A) UC1; B) UC2 and; C) UC3	S6
Figure S4. TEM images of A) UC4; B) UC5, C) UC6 and; D) UC7. Inset in figure S2C correspond to electron diffraction of red squared area	S7
Figure S5. Absorption spectra of CF-OE (0.5 mM) in the presence of increasing amounts of formic acid (% v/v). Inset: zoom image.	S8
Figure S6. A) Transient absorption spectrum (TAS, $\lambda_{\text{exc}} = 355 \text{ nm}$) for CF in deaerated dichloromethane solution immediately after the laser pulse and B) upon 100 ns for CF (red), CF-OE (black) or CF-OE in acidic media (blue) in deaerated dichloromethane solutions. Inset: decay trace monitored at 650 nm for CF-OE as model	S9
Figure S7. A and B) HPLC chromatograms for CF (A) and CF-OE (B) upon increasing concentration in aerated 70:50 $\text{H}_2\text{O} : \text{CH}_3\text{CN}$, containing 0.1% of FA. Inset: corresponding linear calibration curve. C and D) Calibration curve for CF (C) and CF-OE (D). The measurements were performed by triplicated for each compound	S10
Figure S8. HPLC chromatograms of the evolution formation of free CF (red) and disappearance of CF-OE compound (blue) upon increasing irradiation times ($\lambda_{\text{exc}} = 980 \text{ nm}$), at 0.5 M of CF-OE in deaerated methylene chloride (10 % FA v/v). The mobile phase used in HPLC analysis was 70:50 $\text{H}_2\text{O}:\text{CH}_3\text{CN}$, containing 0.1% of FA	S11
Figure S9. HPLC chromatograms of the formation of the benzophenone (BP) as a second product upon increasing irradiation times ($\lambda_{\text{exc}} = 980 \text{ nm}$), at 0.5 mM of CF-OE in deaerated methylene chloride (10 % FA v/v). The mobile phase used in HPLC analysis was 70:50 $\text{H}_2\text{O} : \text{CH}_3\text{CN}$, containing 0.1% of FA. The orange trace corresponds to the commercial BP reference	S12
Figure S10. Reusability of UC3 by monitoring the conversion rate of the formation of CF upon increasing irradiation times ($\lambda_{\text{exc}} = 980 \text{ nm}$) during five consecutive cycles. Cycle 1 to 5: black, red, blue, green and purple, respectively	S13



Scheme S1. Synthetic route for the dyads ciprofloxacin **CF 1** and its corresponding oxime-ester derivative **CF-OE 2**.

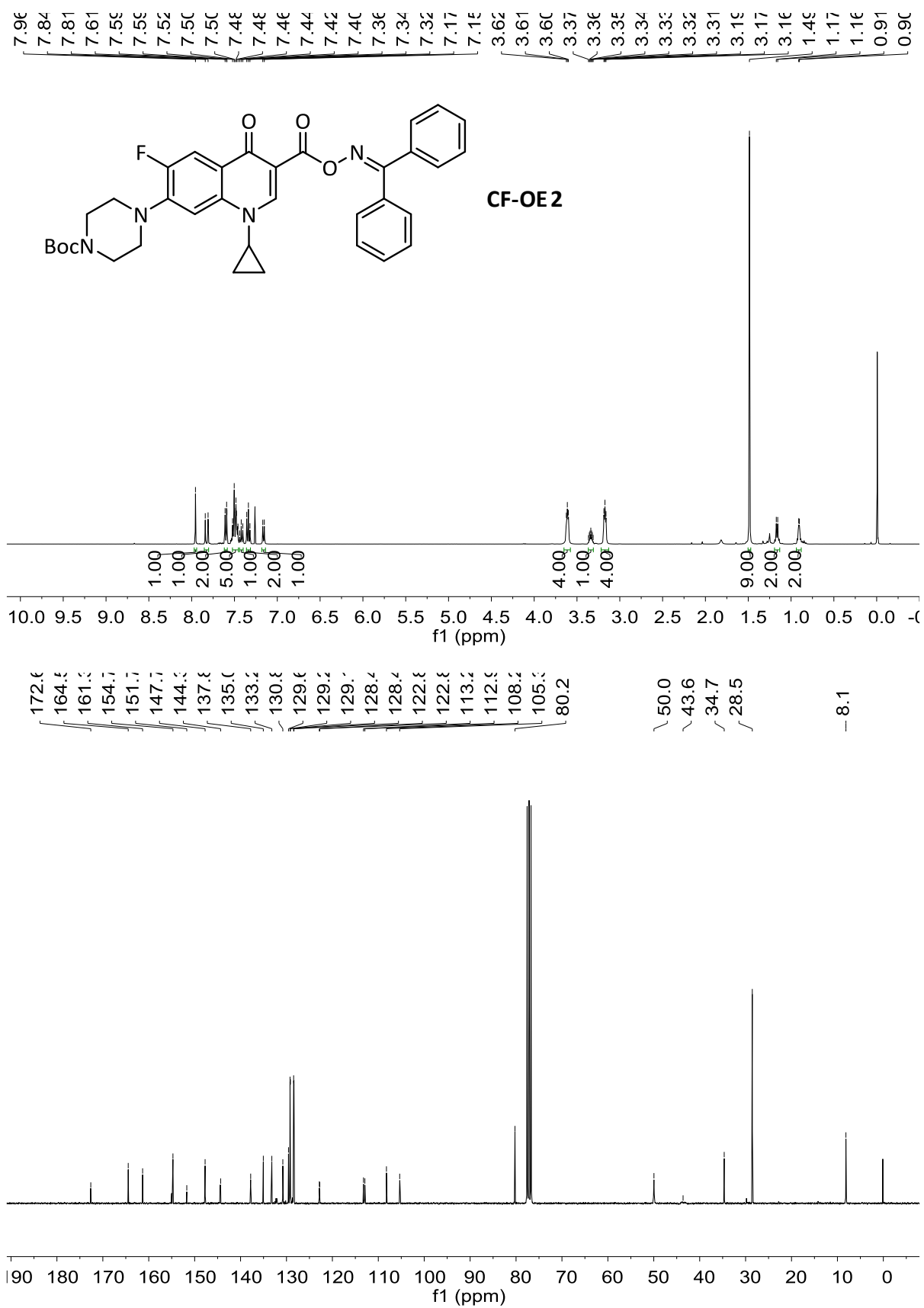


Figure S1. ¹H (up) and ¹³C (down) NMR of **CF-OE 2**

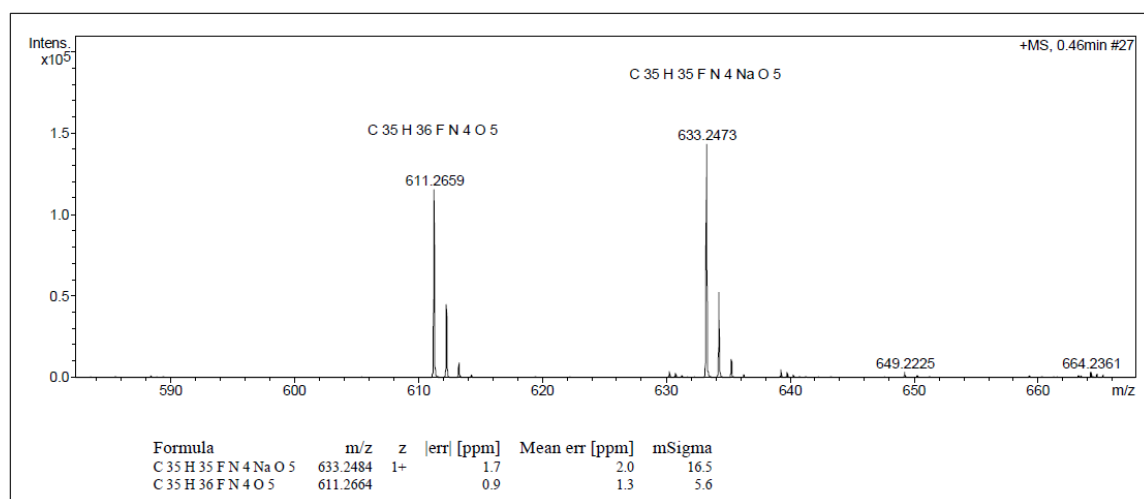


Figure S2. Mass spectrometer characterization data of **CF-OE 2**.

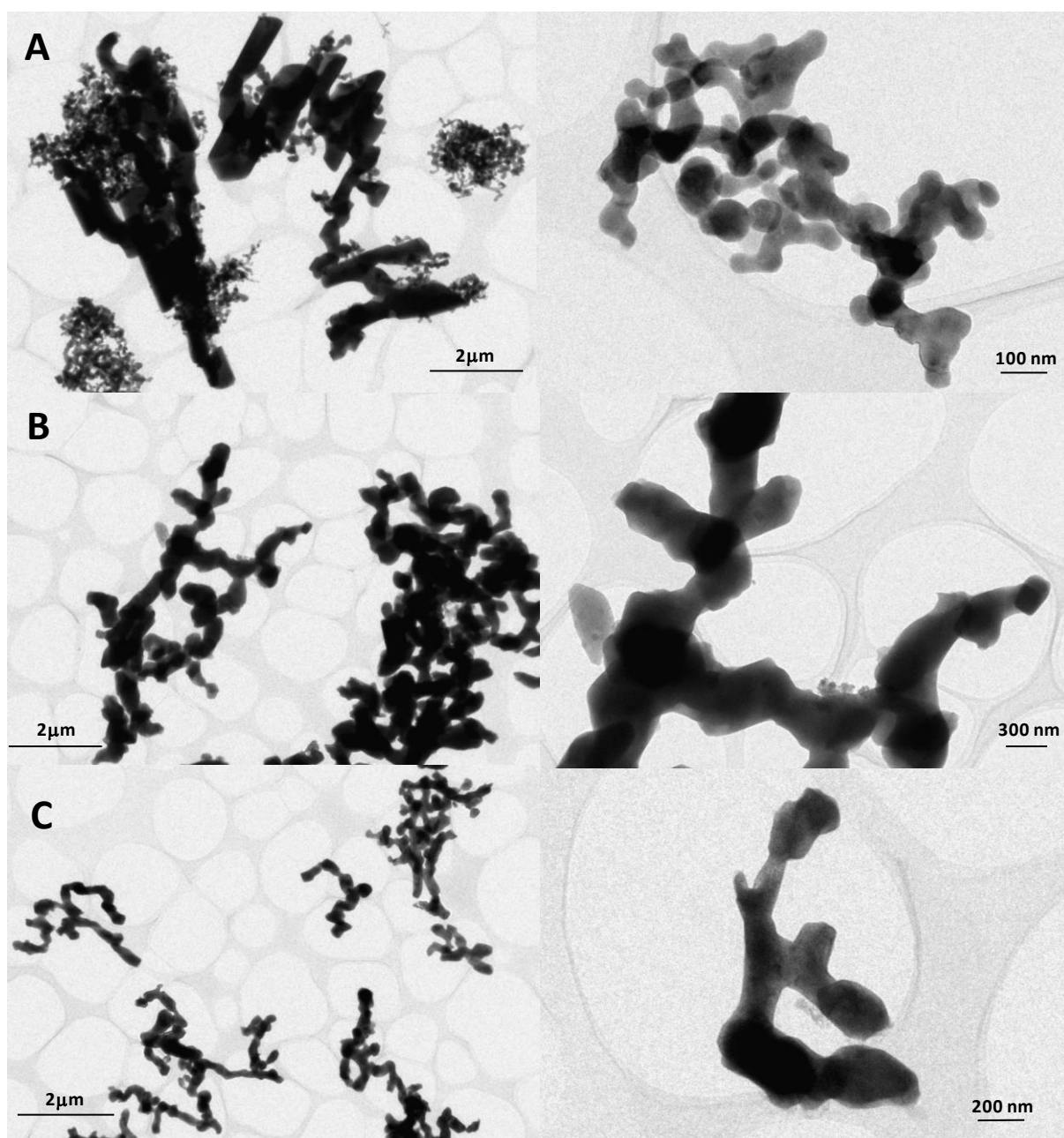


Figure S3. TEM images of A) UC1; B) UC2 and; C) UC3

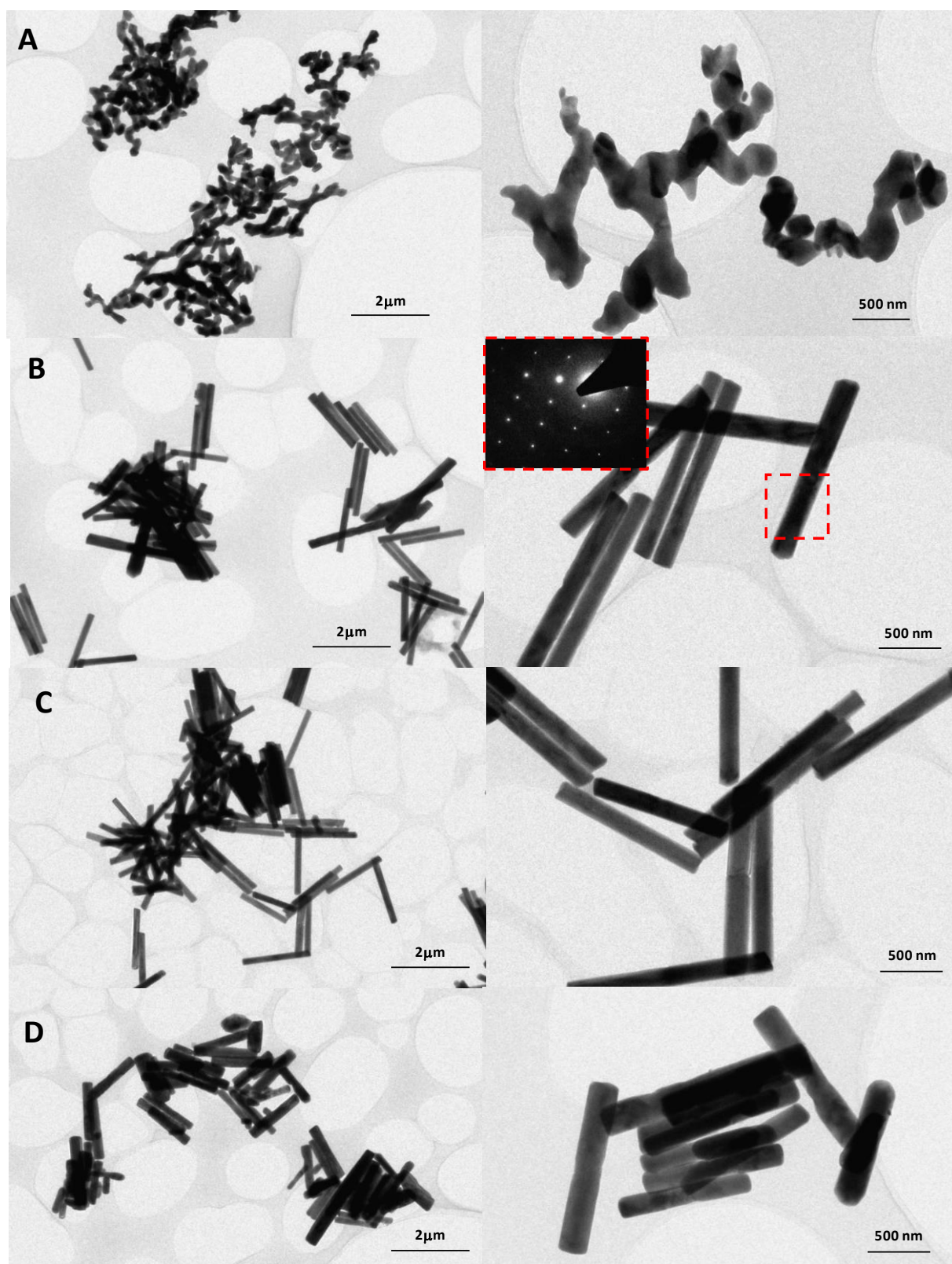


Figure S4. TEM images of A) UC4; B) UC5, C) UC6 and; D) UC7. Inset in figure S2C correspond to electron diffraction of red squared area.

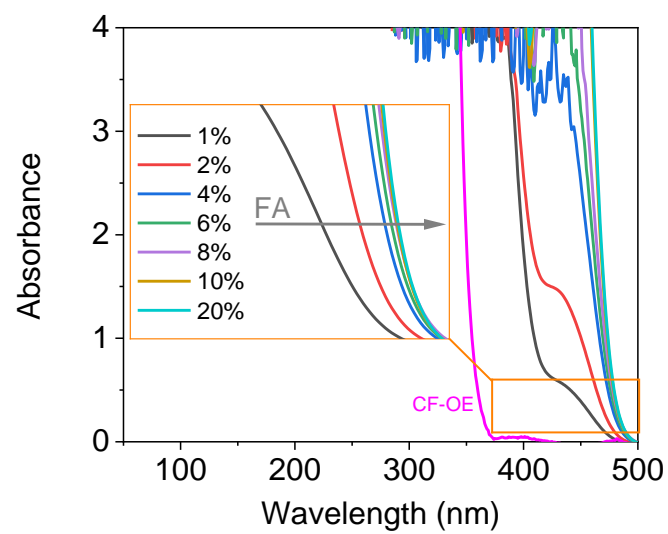


Figure S5. Absorption spectra of CF-OE (pink, 0.5 mM) in the presence of increasing amounts of formic acid (% v/v). Inset: zoom image.

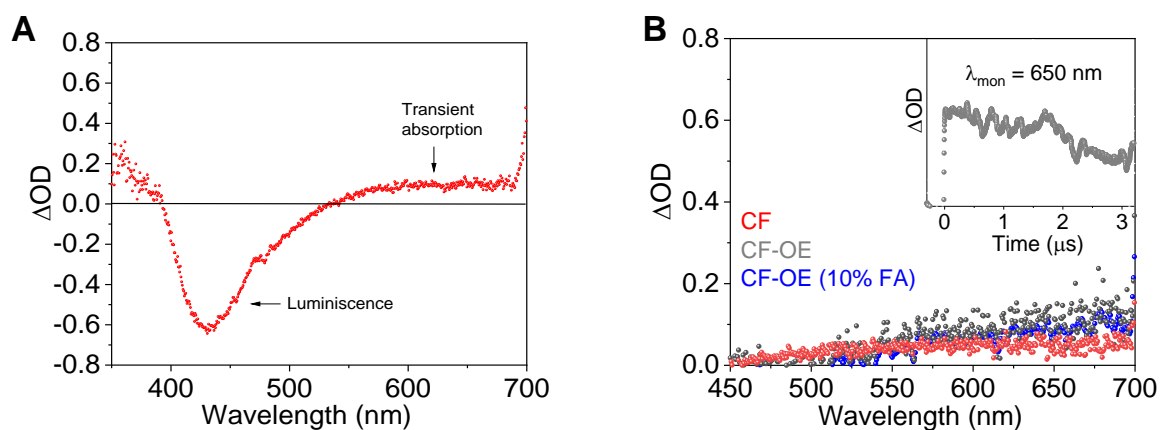


Figure S6. A) Transient absorption spectrum (TAS, $\lambda_{exc} = 355$ nm) for CF in deaerated dichloromethane solution immediately after the laser pulse and B) upon 100 ns for CF (red), CF-OE (black) or CF-OE un acidic media (blue) in deaerated dichloromethane solutions. Inset: decay trace monitored at 650 nm for CF-OE as model.

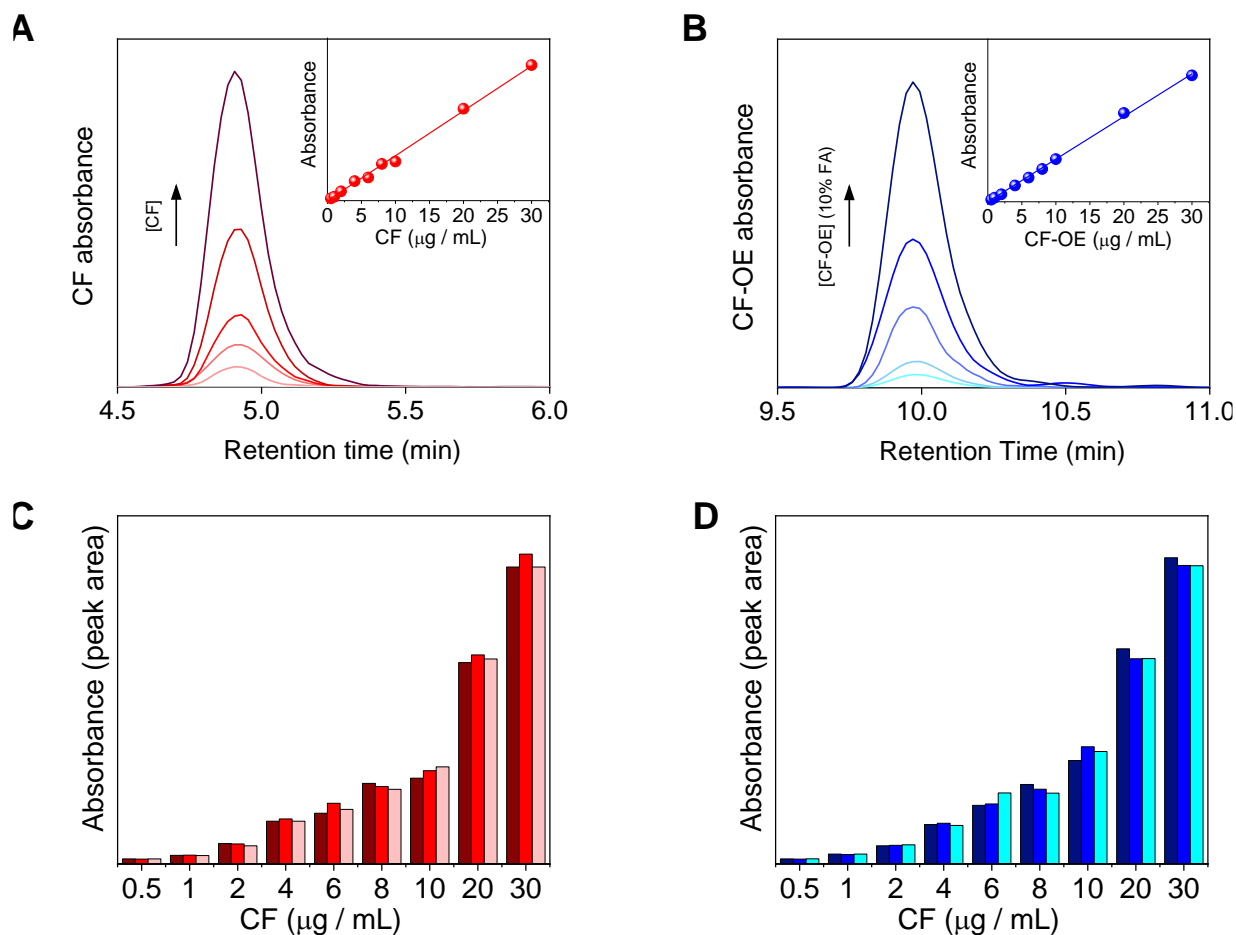


Figure S7. A and B) HPLC chromatograms for CF (A) and CF-OE (B) upon increasing concentration in aerated 70:50 $\text{H}_2\text{O} : \text{CH}_3\text{CN}$, containing 0.1% of FA. Inset: corresponding linear calibration curve. C and D) Calibration curve for CF (C) and CF-OE (D). The measurements were performed by triplicated for each compound.

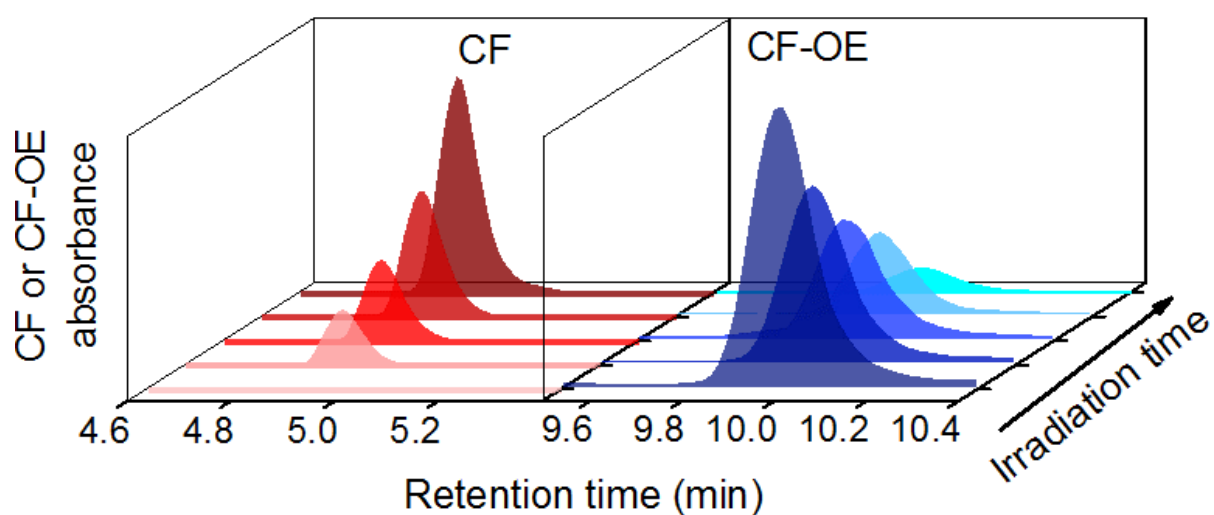


Figure S8. HPLC chromatograms of the evolution formation of free CF (red) and disappearance of CF-OE compound (blue) upon increasing irradiation times ($\lambda_{\text{exc}} = 980$ nm), at 0.5 M of CF-OE in deaerated methylene chloride (10 % FA v/v). The mobile phase used in HPLC analysis was 70:50 H₂O : CH₃CN, containing 0.1% of FA.

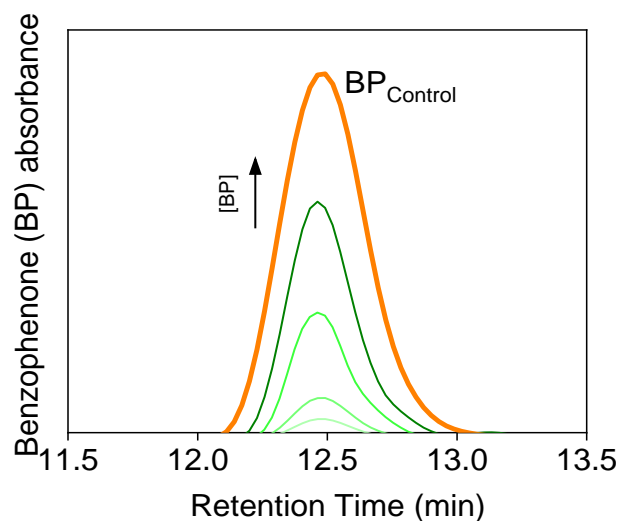


Figure S9. HPLC chromatograms of the formation of the benzophenone (BP) as a second product upon increasing irradiation times ($\lambda_{\text{exc}} = 980 \text{ nm}$), at 0.5 mM of CF-OE in deaerated methylene chloride (10 % FA v/v). The mobile phase used in HPLC analysis was 70:50 H₂O : CH₃CN, containing 0.1% of FA. The orange trace corresponds to the commercial BP reference.

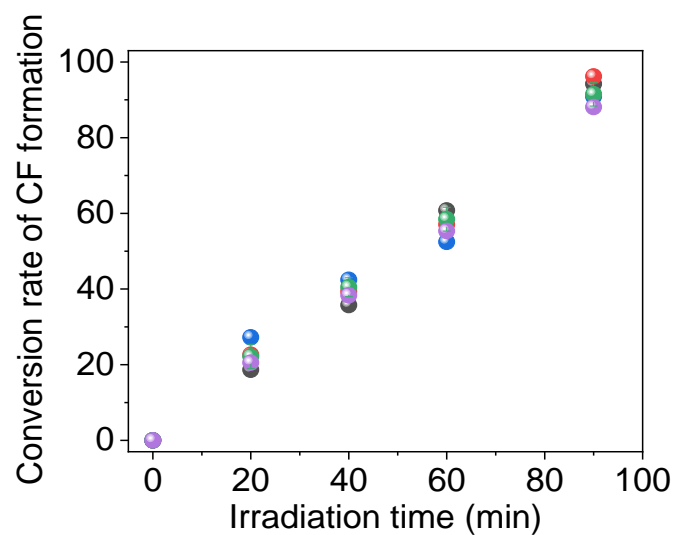


Figure S10. Reusability of UC3 by monitoring the conversion rate of the formation of CF upon increasing irradiation times ($\lambda_{\text{exc}} = 980 \text{ nm}$) during five consecutive cycles. Cycle 1 to 5: black, red, blue, green and purple, respectively.